

Ultimate Load Analysis of Prestressed and Reinforced Concrete Box Culverts

N. MEAMARIAN, T. KRAUTHAMMER, AND JOHN O'FALLON

The effects of compressive membrane forces on the analysis and design of prestressed/reinforced concrete box culverts are considered. Box culvert panels are modeled as one-way slab strips with restrained edges, and the theory of plasticity is applied to find the ultimate load and support reactions for the model. Modified compression field theory is used to relate the sectional forces to internal stress, strain, and angle of diagonal cracks at each specified location and to the total deflection. A direct solution of the equations obtained is not possible. Therefore, numerical methods are used in developing a computer program to perform the calculations. The output results for 16 one-way slab strips are compared with test results. Reasonable agreements are found for load, deflection, and support reactions at the ultimate load conditions. Load enhancement is obtained by considering the ratio of calculated ultimate load to Johansen's load and is found to be between 1.8 and 2.9 for the slabs tested.

Culverts are transverse drains under highway, railroad, and other embankments, made from a variety of materials including reinforced concrete, corrugated metal, plastics, wood, and stone. Cast-in-place or precast reinforced concrete box culverts are very common nationwide. Single or multicell box culverts often provide a cost-effective alternative to short-span low-rise bridges. Box culverts have several advantages over bridges, including lower initial and maintenance expense, less construction time, and simplicity of construction. Precast reinforced concrete box culverts offer additional advantages such as enhanced quality control, use of higher-strength concrete, lower cost because of mass production, shorter installation time, and fewer construction problems related to bad weather.

Several investigations (1-4) suggested that culverts are over-designed. Although applied soil pressure on the culverts has been increased in the latest editions of AASHTO specifications, soil-structure interaction and the effects of compressive membrane forces on structural behavior are still ignored. Current practice for analysis and design of prestressed and reinforced concrete slabs and box culverts is based on elastic methods of analysis and the strength method of design (5; ACI 318-89, ASTM C789-90, ASTM C850-90). Other acceptable methods of analysis and design are not fully developed by standard codes of practice. The standard design tables, based on elastic analysis and ultimate strength design (ASTM C789-90 and ASTM C850-90), are the most widely used method for box culvert design.

Current reinforced concrete models are unable to predict the behavior of cracked concrete members. Most current codes of practice are based on the empirical equations obtained for specific conditions. Furthermore, the artificial division of concrete members into prestressed concrete and conventionally reinforced concrete

makes the codes more complicated and less consistent. There is a need for a rational model to predict the behavior of prestressed/reinforced concrete flexural members under the combined effects of transverse loads and membrane forces induced by edge restraints at the ultimate load condition. Considering the amount of money spent annually for culvert construction, any improvement in design could have a large impact on the annual costs of highway culverts.

MEMBRANE FORCES IN SLABS

Compressive membrane forces, resulting from the lateral support restraints, enhance the flexural strength of slabs (6). A typical load-central deflection curve for an edge-restrained uniformly loaded slab is shown in Figure 1.

There are no membrane forces if no edge restraints are provided, and the slab will fail theoretically at the Johansen's yield line load, as indicated by the dashed line. Compressive membrane forces increase the load capacity of the slab up to Point D on the curve, which will be referred to as the ultimate load of the slab from now on. The ultimate load (also called collapse load) in this paper refers to the nominal load strength of the slab. Provisions of ACI 318-89 Chapter 9 and concept of strength reduction factor, ϕ , must be used to satisfy the design requirements for practical design.

$$\phi(\text{nominal load strength} \geq \text{factored load}, U)$$

Increasing the deflection beyond Point D will cause a sharp decline in the capacity because of the reduction of compressive membrane forces. Starting from Point E, all the membrane forces in the slab change from compression to tension. Tensile membrane forces are carried largely by the reinforcing steel acting as a tensile membrane. The slab will experience large deflections and extensive cracks over the yielded sections in the tensile membrane domain until complete collapse due to reinforcement rupture or debonding of the bars at Point F.

The length of a reinforced concrete box culvert is considerably greater than its width or rise for most practical cases; therefore, each culvert panel can be modeled as one-way slab strips or beams spanning the supports. Considering the preceding rationale, Krauthammer et al. (8) used the Park and Gamble (6) approach for a fixed-end one-way slab strip with four plastic hinges and developed a computer program to obtain a relationship between the normalized central deflection of culvert panels (central deflection/strip depth) and normalized load, with respect to the Johansen's load for different surrounding stiffness values as shown in Figure 2.

1. The ultimate load of a culvert panel is not very sensitive to the exact value of its central deflection.
2. Stiffness of surrounding members need not be very large to provide membrane action.
3. Load enhancement due to membrane action could be more than 50 percent compared with Johansen's yield line theory.

APPROACH

Global Load-Deflection Relationship

Culvert panels can be modeled as one-way slab strips spanning between other panels as the supports (Figure 3). Lateral stiffness of supports and surrounding soil provides the restraint required to develop in-plane forces. Generally, two major steps are required for analysis of this model. First, external analysis is needed to find support reactions, deflections, and applied load. In the second step, reactions and external loads are related to internal stresses of concrete and steel at different locations. Classical methods of analysis are not applicable for this case, since load and support reactions are dependent on material properties, vertical deflection, lateral stiffness of supports, and long-term deformations.

Perhaps the most commonly accepted approach for considering the membrane forces in reinforced concrete slabs is the one presented by Park and Gamble (6), which has been the basis for many other research studies. Four plastic hinges are assumed for the general case to develop a collapse mechanism condition in this method (Figure 4).

Considering the theory of plasticity, equilibrium, and compatibility, Park and Gamble presented an equation to relate the load capacity of the slab strip to its geometry, material properties, lateral shortening, central strip deflection, and lateral stiffness of supports. Park and Gamble's equations can be modified to consider the effects of prestressing force and long-term deformations (9). The free body diagram of Segment 1-2 at and after yielding is considered (Figure 5). Forces applied by each component of the concrete section including reinforcing bars, prestressing tendons, and concrete are shown.

It is assumed that the slab segments between the plastic hinges remain straight after collapse and that there is complete symmetry regarding geometry, reinforcement, loading, and deformations. The supports are assumed to be fixed against rotation and partially

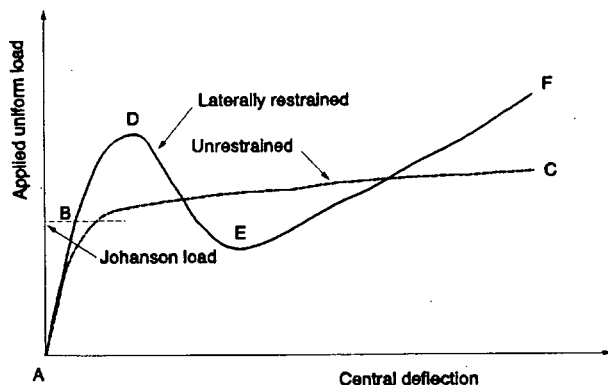


FIGURE 1 Typical load-deflection curve for edge-restrained slabs (7).

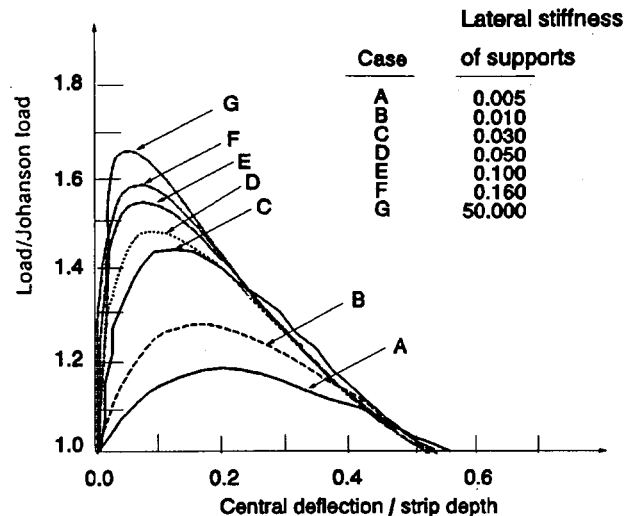


FIGURE 2 Analytical results for ultimate load of bottom slab in a reinforced concrete box culvert (8).

restrained against lateral movements at each end. However, there will be some provision to consider measured rotations as input for the computer program developed herein. Both mild steel reinforcement and prestressing tendons are assumed to have a definite yield point beyond which no extra strength is demonstrated due to strain hardening. Therefore, forces provided by steel at plastic hinges are simply equal to reinforcement areas multiplied by their yield strength. The concepts of Whitney's rectangular stress block (ACI 318-89) for a reinforced concrete section at the ultimate load condition is used to define the sum of the concrete compressive forces at each plastic hinge. It is further assumed that the axial strain, ϵ , is constant along the length of the strip. Application of the equations of equilibrium to the free body diagram shown in Figure 5 will result in the following equation (9):

$$\begin{aligned}
 M_u' + M_u - N_u \delta = & 0.85 f_c' \beta_1 h b \left[\frac{h}{2} \left(1 - \frac{\beta_1}{2} \right) \right. \\
 & + \frac{\delta}{4} (\beta_1 - 3) + \frac{\beta L^2}{48} (\beta_1 - 1) \left(\epsilon + \frac{2t}{L} \right) \\
 & + \frac{\delta^2}{8h} \left(2 - \frac{\beta_1}{2} \right) + \frac{\beta L^2}{4h} \left(1 - \frac{\beta_1}{2} \right) \left(\epsilon + \frac{2t}{L} \right) \\
 & - \frac{\beta_1 \beta^2 L^4}{16 h \delta^2} \left(\epsilon + \frac{2t}{L} \right)^2 \left. \right] - \frac{1}{3.4 f_c' b} (T' + R' - T \\
 & - R - C' + C_t)^2 + (C' + C_t) \left(\frac{h}{2} - d' - \frac{\delta}{2} \right) \\
 & + (T' + T) \left(\frac{h}{2} - d' + \frac{\delta}{2} \right) \\
 & + R' \left(d' - \frac{h}{2} + \frac{\delta}{2} \right) + R \left(d' - \frac{h}{2} + \frac{\delta}{2} \right)
 \end{aligned} \quad (1)$$

where

M_u, M_u' = positive and negative plastic moments, respectively;
 N_u = axial force at ultimate load condition;
 δ = deflection of the middle slab segment;

- f'_c = 28-day concrete uniaxial compressive cylinder strength;
 β_1 = ratio of the equivalent stress block depth to neutral axis depth;
 h = member thickness;
 b = beam or slab strip width;
 β = ratio of the positive hinge distance from support to the member span length;
 L = length of span;
 ϵ = axial short-term strain;
 t = outward lateral movement of each support;
 T, T' = steel tensile forces at positive and negative hinges, respectively;
 R, R' = prestressing tensile forces at positive and negative hinges, respectively;
 C_s, C'_s = compressive steel forces at positive and negative hinges, respectively;
 d' = concrete cover to the center of mild steel reinforcement;
 d, d' = top and bottom cover to the center of prestressing steel at positive and negative hinges, respectively; and
 c, c' = depth of neutral axis at positive and negative hinges, respectively.

The term $\epsilon + 2t/L$ on the right-hand side of Equation 1, which is the total axial strain, can be found as shown below (9), where S is the support lateral stiffness per unit width of the slab strip or beam at each end [e.g., load per unit of outward displacement of the support in units of (lb/in.)/in], E_c is the concrete modulus of elasticity, and K is the ratio of long-term to short-term deformations. Note that the Park and Gamble equations may be obtained by inserting the values of $b = 1$ and $R' = R = K = 0$.

$$\epsilon + \frac{2t}{L} = \frac{\left(\frac{1+K}{hE_c} + \frac{2}{LS}\right) \left[0.85f'_c \beta_1 \left(\frac{h}{2} - \frac{\delta}{4} - \frac{T' + R' - T - R - C'_s + C_s}{1.7f'_c \beta_1 b} \right) + \frac{C_s - T - R}{b} \right]}{1 + 0.2125 \frac{f'_c \beta_1 \delta L^2}{\delta} \left(\frac{1+K}{hE_c} + \frac{2}{LS} \right)} \quad (2)$$

A relationship can be found between the external loads and sum of the internal moments about Point 2 in Figure 5 (interior hinge)

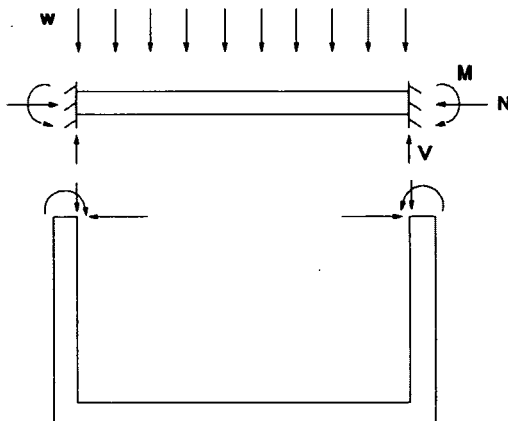


FIGURE 3 Modeling of box culverts.

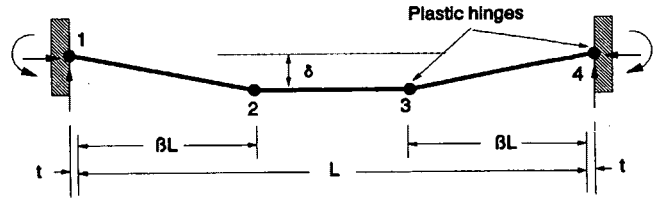


FIGURE 4 Plastic hinges in restrained slab strip (6).

by using the principles of virtual work. The internal virtual work done by Segment 1-2 of the slab strip due to a virtual rotation of θ about Point 1 is equal to $(M_u + M'_u - N_u \delta)\theta$. Equating the external and internal virtual work for Segment 1-2 leads to Equation 3 for a uniformly distributed load and Equation 4 for two concentrated loads of P and βL from each end:

$$\left(\frac{w}{2}\right) (\beta L)^2 = M_u + M'_u - N_u \delta \quad (3)$$

$$P(\beta L) = M_u + M'_u - N_u \delta \quad (4)$$

A direct solution of Equations 3 or 4 is not possible, since there is only one equation with two unknowns (w or P and δ). An iterative numerical solution is adopted in which the value of δ is increased gradually. For each value δ_i , the corresponding value of the applied load, w_i or P_i , is obtained by using Equations 1, 2, and 3 or 4 according to the loading type. The iteration process continues until an appropriate ultimate load and the corresponding deflection are obtained (Point D in Figure 1). Then support reactions can be found by applying equations of equilibrium and strain compatibility (9). Sectional forces at any point between the supports can be calculated by using equilibrium equations when the end reactions are obtained.

Consideration of Internal Conditions

The recently developed modified compression field theory, fully explained by Vecchio and Collins (10-12) and Collins and Mitchell (13), provides a unified approach for the analysis of reinforced concrete sections under combined effects of shear, moment, and axial loads. Modified compression field theory is applicable to reinforced and prestressed concrete flexural members at different stages of loading and cracked concrete condition. It is assumed that shear forces are resisted by a field of diagonal compressive stress, f_2 (Figure 6), with angle of θ , in combination with a field of diagonal tensile stress, f_1 . Mohr's circle relates the principal strains to the angle of inclination of the cracks, θ , and to the longitudinal and transverse strains (strain compatibility). Material stress-strain relationships are used to relate strains in each material to stresses, and equilibrium equations are applied to find the relationship between the internal stresses and sectional forces resulting from the external loads (13). Equations of the modified compression field theory are not suitable for direct solution without more simplification. Therefore, an iterative method of solution is adopted in this study by using numerical solution techniques and computer programming (9,13). This method involves three major nested loops (iterating loops) based on concrete tensile strain, ϵ_t , shear force, V , and crack inclination angle, θ .

Material Constitutive Laws

Material constitutive laws will be satisfied by considering the stress-strain relationship for steels and concrete. Mild steel reinforcement is assumed to act as an elastic-plastic material in tension or compression. In practice, the stress-strain curve for prestressing steel is linear before the elastic limit, at about $0.7f_{pu}$. This relationship is approximated by a Ramberg-Osgood curve, as defined below (14):

$$f_p = E_p \epsilon_p \quad f_p \leq 0.7f_{pu} \quad (5)$$

$$f_p = \frac{E'_p \epsilon_p}{\left[1 + \left(\frac{E'_p \epsilon_p}{f_{pu}} \right)^{1/m} \right]} \quad f_p > 0.7f_{pu} \quad (6)$$

where E'_p is the tangential modulus of the Ramberg-Osgood curve and m is the shape parameter (taken as 4).

The compressive stress-strain curve for concrete is usually obtained from the standard cylinder compressive test, but stress conditions in a cracked concrete section are quite different from the cylinder test. Vecchio and Collins (10) found that the principal compressive stress of concrete, f_2 , depends not only on the principal compressive strain, ϵ_2 , but on the principal tensile strain, ϵ_1 , as well. They suggested the following parabolic stress-strain relationship for normal strength [$f'_c < 6,000$ psi (41.38 MPa)] cracked concrete:

$$f_2 = f_{2max} \left[2 \left(\frac{\epsilon_2}{\epsilon'_c} \right) - \left(\frac{\epsilon_2}{\epsilon'_c} \right)^2 \right] \quad (7)$$

$$\frac{f_{2max}}{f'_c} = \frac{1}{0.8 + 170\epsilon_1} \leq 1.0 \quad (8)$$

where

- f_{2max} = cracked concrete compressive strength,
- ϵ'_c = concrete cylinder strain at compressive strength,
- ϵ_1 = concrete tensile strain, and
- ϵ_2 = concrete compressive strain.

An equation for concrete of higher strength has been suggested by Thorenfelt et al. (15). The equation is a generalization of two of the expressions recommended by Popovics (16). This equation

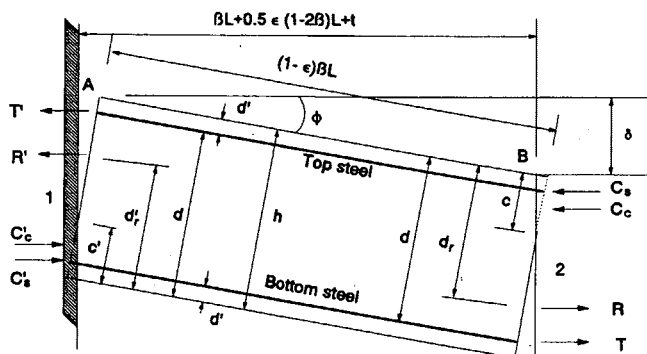


FIGURE 5 Deformed shape and forces for a slab segment between the plastic hinges (6).

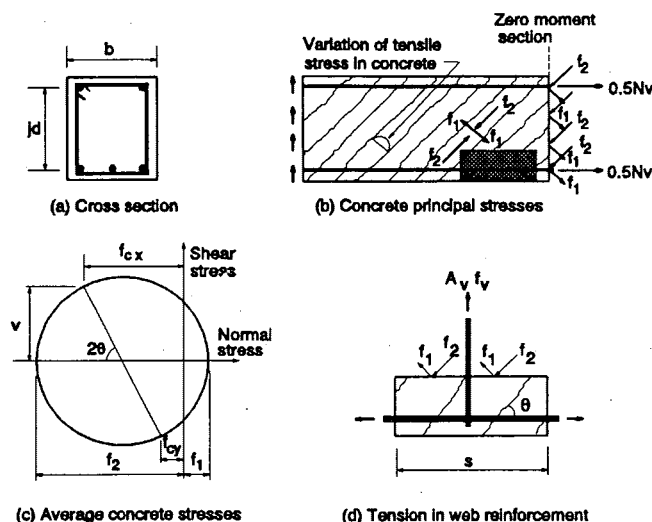


FIGURE 6 Equilibrium conditions for modified compression field theory (13).

relates the concrete stress, f'_c , to concrete strain, ϵ_2 , as follows:

$$\frac{f'_c}{f'_c} = \frac{n_f \left(\frac{\epsilon_2}{\epsilon'_c} \right)}{n_f - 1 + \left(\frac{\epsilon_2}{\epsilon'_c} \right)^{n_f k_d}} \quad (9)$$

where

- ϵ'_c = concrete cylinder strain at compressive strength $\approx (f'_c/E_c) \times [n_f/(n_f - 1)]$,
- n_f = curve-fitting factor $= E_c/(E_c + E'_c) \approx 0.8 + f'_c/2,500$ (f'_c in psi),
- E_c = concrete tangent modulus of elasticity when $\epsilon_c = 0$,
- $E'_c = f'_c/\epsilon'_c$, and
- k_d = factor to increase the stress decay after the ultimate strength, taken as 1 for $\epsilon_2/\epsilon'_c < 1$ and $k_d \approx 0.67 + f'_c/9,000$ for $\epsilon_2/\epsilon'_c > 1$ (f'_c in psi).

Collins and Mitchell (13) modified the recommended average tensile stress curve for concrete, given by Vecchio and Collins (11), to account for the effects of steel bond and loading type (Equations 10 and 11):

$$f_1 = E_c \epsilon_1 \quad \epsilon_1 \leq \epsilon_{cr} \quad (10)$$

$$f_1 = \frac{\alpha_1 \alpha_2 f_{cr}}{1 + \sqrt{500\epsilon_1}} \quad \epsilon_1 > \epsilon_{cr} \quad (11)$$

where

- ϵ_1 = average concrete principal tensile strain between the diagonal cracks,
- f_1 = average concrete principal tensile stress between the diagonal cracks,
- ϵ_{cr} = concrete cracking strain,
- f_{cr} = concrete cracking strength,
- α_1 = reinforcement bond characteristics factor, and
- α_2 = loading type factor.

Shear capacity of a concrete member may be limited to the forces transmitted along the cracks. Local shear forces transmitted by aggregate interlock are dependent on the crack width. Collins and Mitchell (13) suggested a simplified form of the equation given by Vecchio and Collins (11) for the limiting value of the local shear stresses along the cracks, v_{ci} , as below (in psi), where ω is the crack width calculated according to CEB-FIP code (in.) (17) and a = maximum aggregate size (in.).

$$v_{ci} = \frac{2.16\sqrt{f'_c}}{0.3 + \frac{24\omega}{a + 0.63}} \quad (12)$$

Since the two sets of forces shown at Sections 1-1 and 2-2 in Figures 7b and 7c must be statistically equivalent, they have the same sum of vertical components. With the assumption of shear reinforcement yielding at cracks, the equality mentioned above yields Equation 13:

$$f_1 = v_{ci} \tan \theta + \frac{A_v}{sb} (f_{vy} - f_v) \quad (13)$$

where f_{vy} and s are shear reinforcement yield strength and spacing, respectively. The smallest value from Equations 10, 11, and 13 is considered to be the concrete principal tensile strength.

Stress and strain conditions become more complex after the section is cracked. The presence of concrete tensile stresses between the cracks stiffens the member. This phenomenon, which is called tension stiffening, is accounted for by using the average tensile stress given by Equation 11 and is considered to exist only around the tensile reinforcement in an area called the effective embedment zone (12). The effective embedment zone is assumed to be extended $7.5 d_b$ in each direction parallel to the sides of the section around each longitudinal tensile reinforcing bar, where d_b is the bar diameter (17).

Numerical Implementation

A computer program has been developed for IBM-PC and compatible computers based on a 20-step iterative solution technique

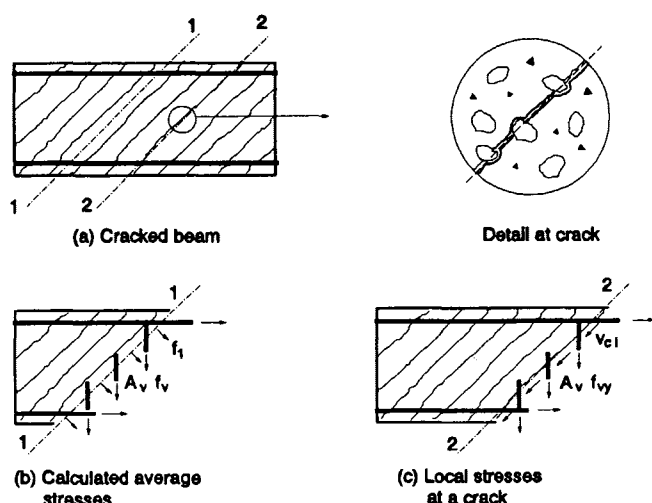


FIGURE 7 Stress transmission across the cracks (13).

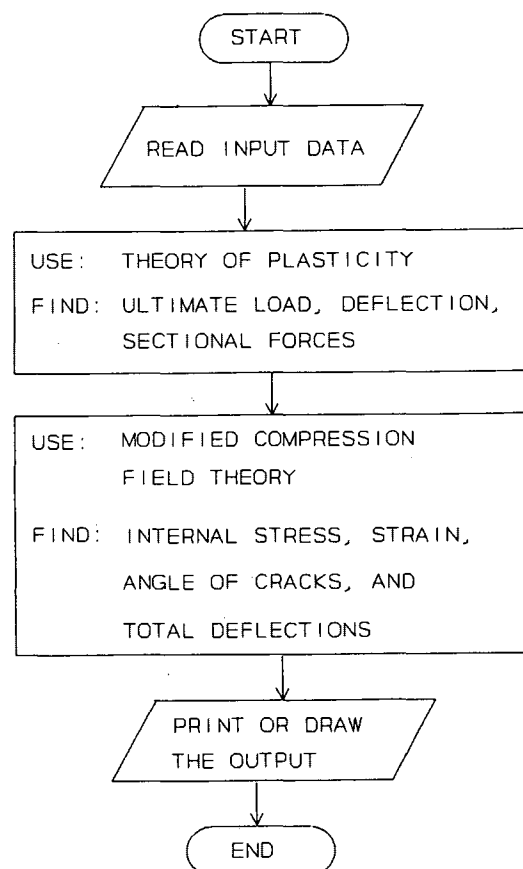
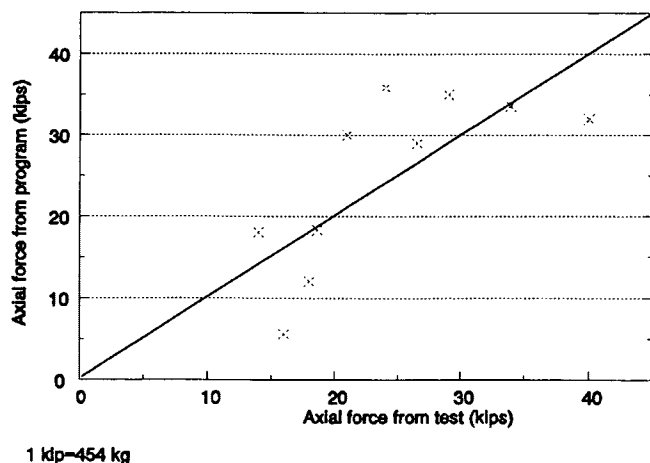


FIGURE 8 Condensed flowchart.

(9). A condensed flowchart for the program is shown in Figure 8. Geometry, material properties, reinforcement area, loading type, and so forth are given as input data. Support reactions, deflection, and load at ultimate conditions are then calculated by using an iterative procedure for incremental deflection values (Equations 1 and 2). In the next step, equations of equilibrium are applied to find the sectional forces at any specified section between the supports, after which the principles of the modified compression field theory are applied by using a numerical solution method (9,13) to find all the unknown parameters including stresses and strains in concrete and steel, angle of diagonal cracks, total deflection, and crack width at the ultimate load conditions. The output of the computer program can be used to check the adequacy of a reinforced/prestressed concrete member for structural strength and serviceability. The member geometry or reinforcement area need to be revised if strength or serviceability requirements are not satisfied.

COMPARISON WITH EXPERIMENTAL RESULTS

A series of 16 slab panels 36 in. (914 mm) long by 24 in. (610 mm) wide were tested by Guice (18). Two sets of equal numbers of slab specimens were cast with thicknesses of $2\frac{5}{16}$ in. (59 mm) and $1\frac{5}{8}$ in. (41 mm). The area of main reinforcement was the same for the midspan and the supports but differed from one slab to another. Small-diameter deformed wire was used for both tem-



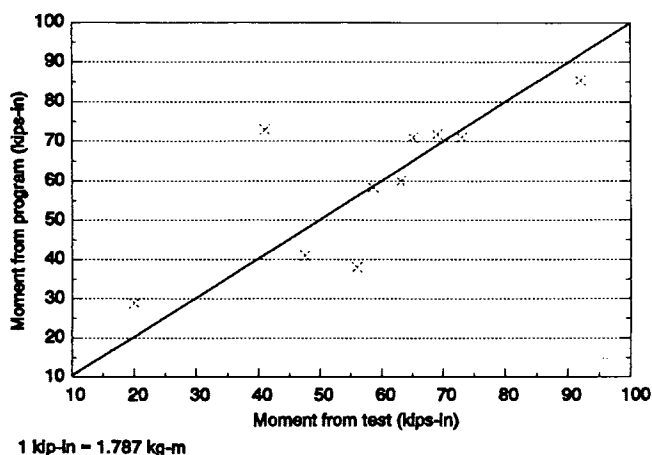
1 kip = 454 kg

FIGURE 9 Computer program versus test (axial force).

perature and shear reinforcements. Pin-shaped shear reinforcement was used at each location of longitudinal and transverse reinforcement contact. The important fact about the testing assembly is that the steel supports for the slabs were designed to allow partial lateral movement and rotation of the supports. Support rotation was not originally considered in the equations obtained from the theory of plasticity for external analysis, but the required provisions were added to the computer program to consider the effects of given support rotations on the external analysis. The values obtained from the computer output for axial force, support moment, load, and deflection/thickness ratio (δ/h) at the ultimate load condition are plotted against the corresponding results from the test data in Figures 9 through 12. The average, standard deviation, and coefficient of variance for the ratio of calculated to test results are given in Table 1.

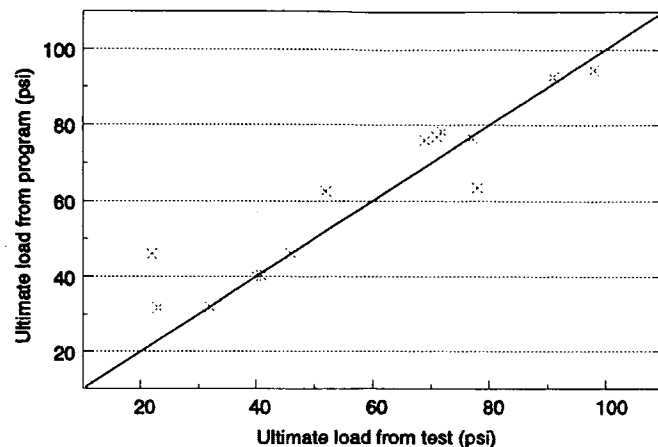
PRESENT APPROACH VERSUS YIELD LINE APPROACH

The yield line theory approach (19) is used to compare the ultimate load of the slab specimens to those resulting from the ap-



1 kip-in = 1.787 kg-m

FIGURE 10 Computer program versus test (support moment).



1 psi = 6.89 kPa

FIGURE 11 Computer program versus test (ultimate load).

plication of the computer program developed in this study. Membrane force is not considered in the yield line theory; thus it does not contribute to the ultimate load capacity obtained by the yield line theory. The ratios of computed load/Johansen's load are plotted against the reinforcement percentage ratio for each group of slab thicknesses in Figure 13. The solid line is for the thicker slabs [$H = 2\frac{5}{16}$ in. (59 mm)], and the dashed line is for the thinner slabs [$H = 1\frac{5}{8}$ in. (41 mm)].

DISCUSSION OF RESULTS

Evaluation of the results in Table 1 and Figures 9 through 12 indicates that program outputs are reasonably close to test results. The average ratio of theoretical load to tested load is only 4 percent higher than 1 with a standard deviation of 0.13. The average values for the ratios of calculated to tested axial force and moment at the supports are 7 percent higher than 1. Whereas the deviations are small and reasonable, they may be due to several factors including support rotation, initial gap between the slab and support

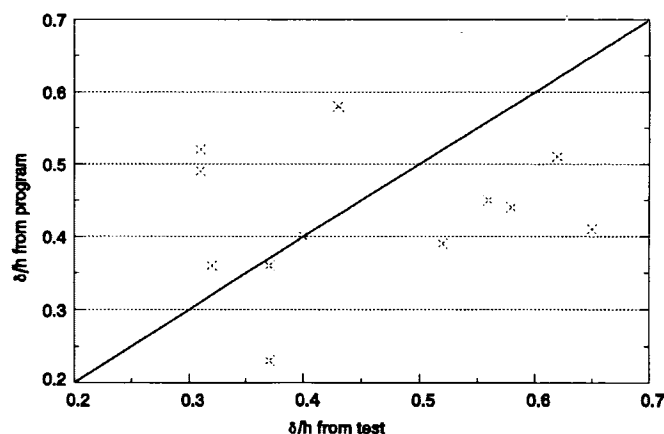


FIGURE 12 Computer program versus test (deflection/thickness).

TABLE 1 Calculated Values and Test Results (Statistical Parameters)

Parameter	Axial Force	Moment	Load	Deflection
Average	1.07	1.07	1.04	1.00
Std. Deviation	0.38	0.29	0.13	0.33
Coefficient of Variance	35%	27%	12%	33%

rack, and debonding. The average theoretical deflection is the same as the average test results. It appears that despite the very close results, theoretical deflections are less than the tested values for higher deflection/thickness ratios due to the same problems discussed above. Evaluation of Figure 13 indicates a considerable load enhancement as expected due to membrane forces, especially for low reinforcement ratios (calculated load/Johansen's load = 1.7 to 2.9). Figure 13 also shows that the load enhancement is higher for thinner slabs with moderate reinforcement ratios (0.007 to 0.012), but it is the same for slabs with low reinforcement ratios (0.005).

Effects of support rotation complicate the analysis. It was assumed that top steel at the supports yields even after the introduction of compressive strains at the top steel level because of support rotation. This assumption is necessary to find the ultimate load from the collapse mechanism; however, this might not be representative of the actual conditions. Testing may have been terminated because of large deflections due to support rotations, before the top support rebars yielded (18). The other problem observed in the test procedure was related to uneven support rotations and forces. This violates the assumption that was made for a symmetrical geometry.

CONCLUSIONS

It was shown that the combined application of the theory of plasticity and the modified compression field theory provides a rational method for prediction of structural response of one-way slabs with laterally restrained edges. The formulations satisfy con-

ditions of equilibrium, compatibility, and plane section theory and give a realistic consideration of cracked concrete behavior. Several critical factors such as strain softening, tension stiffening, repeated load, reinforcement type, and long-term shortening are considered in this approach. This analytical model incorporates the theoretical relationships between parameters in easy-to-use computer software on the basis of numerical iteration methods. Application of the software to 16 reduced-scale one-way reinforced concrete slab panels and comparison with actual test results shows that, overall, the program outputs regarding the forces at the supports, load, and deflection of mid-span at ultimate load condition are reasonably close to test results.

The study considered the membrane forces and arching action for one-way prestressed and reinforced concrete flexural member analysis and design in a rational manner, leading to significant load enhancement and saving of reinforcement and concrete materials in addition to more accurate prediction of member behavior at cracked condition. The results are also applicable to any structure that can be modeled as a one-way member with restrained edges. For example, the strip method can be used to model a two-way slab or box culverts as a series of one-way strips that can be analyzed easily by the software.

RECOMMENDATIONS

It was demonstrated that the presence of compressive membrane force enhances the flexural strength of concrete members considerably; therefore, it is recommended that membrane forces be considered in the analysis and design of flexural prestressed and reinforced concrete structural members with laterally restrained edges, such as box culverts and interior slab panels. The required provisions regarding the consideration of such forces for design purposes need to be included in the prestressed and reinforced concrete design codes. A uniform approach for prestressed and reinforced concrete members and higher values for load factors are recommended until further study, especially for sustained loads. Axial shortening resulting from long-term deformations and outward lateral movement of the supports could reduce the membrane force considerably. Therefore, careful consideration of support lateral stiffness and long-term axial deformation is important to prevent overestimation of flexural enhancement provided by membrane forces.

There is a need for more testing to obtain a better definition of structural behavior and to verify the software output results for stresses and strains and for prestressed elements. It is also desirable to model the D-regions (disturbed regions where stress trajectories are not smooth) at and around plastic hinges and implement this model in the computer program to have a more complete and accurate analysis of the structure. A possible method for modeling D-regions is using the strut-and-tie method (20). The boundary loads and deformations for D-regions can already be obtained from the current program output. Combined application of the present software and proper modeling of D-regions would provide a consistent method of analysis and smooth transition from B-regions to D-regions. The analysis in this study is valid only for symmetrical slabs with regard to reinforcement, geometry, and end restraints. Further study to consider unsymmetrical cases is necessary.

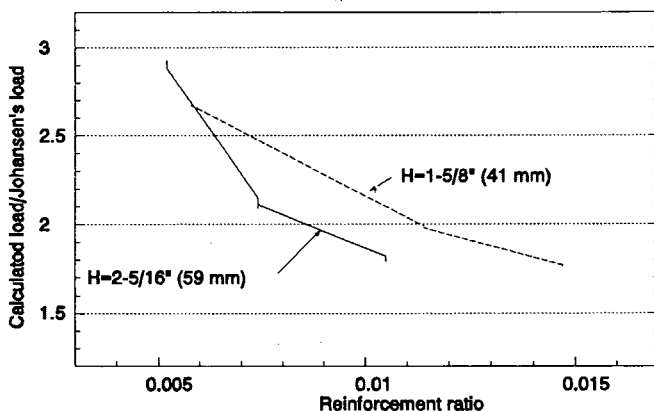


FIGURE 13 Computer program versus yield line theory for tested slabs.

ACKNOWLEDGMENT

This study was sponsored by FHWA. The authors gratefully acknowledge the sponsorship of this organization.

REFERENCES

1. Tadros, M. K., C. Belina, and D. W. Meyer. Current Practice of Reinforced Concrete Box Culvert Design. In *Transportation Research Record 1191*, TRB, National Research Council, Washington, D.C., 1988, pp. 65–72.
2. Katona, M. G., P. D. Vittes, C. H. Lee, and H. T. Ho. CANDE-1980: Box Culverts and Soil Models. Report FHWA-RD-89-172. Federal Highway Administration, 1981.
3. Frederick, G. R., C. V. Ardis, K. M. Tarhini, and B. Koo. Investigation of the Structural Adequacy of C 850 Box Culverts. In *Transportation Research Record 1191*, TRB, National Research Council, Washington, D.C., 1988, pp. 73–80.
4. Tadros, M. K., J. V. Benak, A. M. Abdel-Karim, and K. A. Bexten. Field Testing of a Concrete Box Culvert. In *Transportation Research Record 1231*, TRB, National Research Council, Washington, D.C., 1989, pp. 49–55.
5. *Standard Specification for Highway Bridges* (15th edition). AASHTO, Washington, D.C., 1992, pp. 124–326.
6. Park, R., and W. L. Gamble. *Reinforced Concrete Slabs*. John Wiley and Sons, 1980, pp. 562–565.
7. Iqbal, M., and A. T. Derecho. *Design Criteria for Deflection Capacity of Conventionally Reinforced Concrete Slabs, Phase I*. State-of-the-Art Report, Naval Construction Battalion Center, Port Heuneme, Calif., May 1979.
8. Krauthammer, T., J. J. Hill, and T. S. Fares. Enhancement of Membrane Action for Analysis and Design of Box Culverts. In *Transportation Research Record 1087*, TRB National Research Council, Washington, D.C., 1986, pp. 54–61.
9. Meamarian, N. *Compressive Membrane Effects on the Behavior of One-Way Structural Concrete Members with Application for Analysis and Design of Box Culverts*. Thesis. The Pennsylvania State University, University Park, 1993.
10. Vecchio, F. J., and M. P. Collins. *The Response of Reinforced Concrete to In-Plane Shear and Normal Stresses*. Publication 82-03. Department of Civil Engineering, University of Toronto, Toronto, Ontario, Canada, 1982.
11. Vecchio, F. J., and M. P. Collins. The Modified Compression Field Theory for Reinforced Concrete Elements Subjected to Shear. *ACI Structural Journal*, Vol. 83, No. 2, March–April 1986, pp. 219–231.
12. Vecchio, F. J., and M. P. Collins. Predicting the Response of Reinforced Concrete Beams Using Modified Compression Field Theory. *ACI Structural Journal*, May–June 1988, pp. 258–268.
13. Collins, M. P., and D. Mitchell. *Prestressed Concrete Structures*. Prentice-Hall, Inc., 1991.
14. Hsu Thomas, T. C. Nonlinear Analysis of Concrete Membrane Elements. *ACI Structural Journal*, Vol. 88, No. 5, Sept.–Oct. 1991, pp. 552–561.
15. Thorenfelt, E., A. Tomaszewicz, and J. J. Jensen. Mechanical Properties of High-Strength Concrete and Application in Design. *Proc., Symposium on Utilization of High-Strength Concrete*, Stavanger, Norway, June 1987, pp. 149–159.
16. Popovics, S. A Review of Stress-Strain Relationships for Concrete. *ACI Journal*, Vol. 67, No. 3, 1970, pp. 243–248.
17. *Model Code for Concrete Structures* (3rd. edition). Comité Euro-International du Béton, Paris, 1978.
18. Guice, L. K. *Behavior of Partially Restrained Reinforced Concrete Slabs*. Technical Report SL-86-32. Structures Laboratory, U.S. Army Engineer Waterways Experiment Station, Vicksburg, Miss., Sept. 1986.
19. Johansen, K. W. *Yield Line Formulae for Slabs*. Cement and Concrete Association, London, 1972.
20. Schlaich, J., K. Schäfer, and M. Jennewein. Toward a Consistent Design of Structural Concrete. *PCI Journal*, May–June 1987, pp. 75–150.

The content of this paper reflects views of the authors and the results of their study. The contents are not necessarily official views or policies of FHWA or Pennsylvania State University.

Publication of this paper sponsored by Committee on Culverts and Hydraulic Structures.